Journal of
Materials Chemistry A

Accepted Manuscript

This article can be cited before page numbers have been issued, to do this please use: Q. Sun, X. Li, Q. Lin and M. Lu, *J. Mater. Chem. A*, 2019, DOI: 10.1039/C8TA12506F.

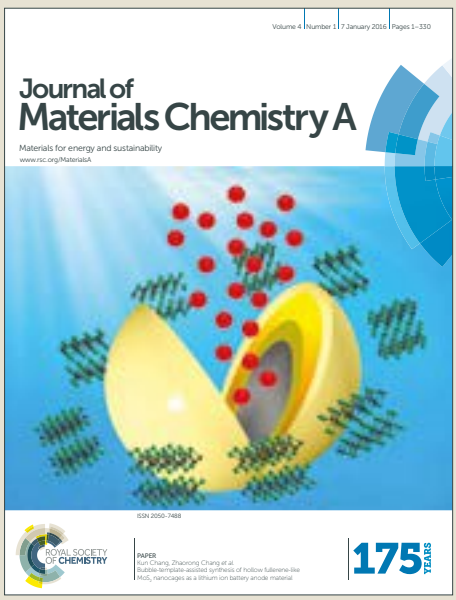

ROYAL SOCIETY OF CHEMISTRY

rsc.li/materials-a

View Article Online
DOI: 10.1039/C8TA12506F

Journal Name

ARTICLE

Dancing with 5-substituted monotetrazoles, oxygen-rich ions, and silver: Towards primary explosives with positive oxygen balance and excellent energetic performance

Received 00th January 20xx,
Accepted 00th January 20xx

DOI: 10.1039/x0xx00000x

www.rsc.org/

Qi Sun, Xin Li, Qiuhan Lin*, and Ming Lu*

Although numerous primary explosives have been reported to date, those with a positive oxygen balance are extremely rare. To overcome this limitation, we present two strategies to improve the oxygen balance: 1) increasing the oxygen balance in the ligands and 2) the introduction of oxygen-rich ions. By applying these strategies, a series of energetic coordination polymers (ECPs) consisting of 5-substituted monotetrazoles, oxygen-rich ions, and silver (*viz* $[Ag_7MT_4(NO_3)_3]_n$, $[Ag_3HT_2NO_3]_n$, $[Ag_7AT_4(NO_3)_3]_n$, $[Ag_5NT_4NO_3]_n$, and $[Ag_5NT_4ClO_4]_n$) were prepared. Their structures were characterized using single crystal XRD, IR, and elemental analysis, and their properties were evaluated in terms of density, thermal stability, mechanical sensitivity and oxygen balance. In addition, the potential structure-property relationships of these polymers were studied. All five ECPs possessed high density ranging from 3.12 to 3.60 g cm^{-3}. DSC and TGA analysis showed that the ECPs have high thermal stability with decomposition temperatures ranging from 251 to 348 °C. All the ECPs were sensitive to stimulus and should be classified as primary explosives. Oxygen balance calculations, detonation reactions, and combustion experiments showed that $[Ag_5NT_4NO_3]_n$ and $[Ag_5NT_4ClO_4]_n$ have a positive oxygen balance, which gives the first two examples of ECPs-based primary explosives exhibiting a positive oxygen balance (based on CO_2). Explosion experiments showed that $[Ag_5NT_4NO_3]_n$ and $[Ag_5NT_4ClO_4]_n$, which display a positive oxygen balance, deliver improved initiation performance when compared to $[Ag_7MT_4(NO_3)_3]_n$, $[Ag_3HT_2NO_3]_n$, and $[Ag_7AT_4(NO_3)_3]_n$, which have a negative oxygen balance. Therefore, $[Ag_5NT_4NO_3]_n$ and $[Ag_5NT_4ClO_4]_n$ are efficient primary explosives. In addition, the positive oxygen balance of $[Ag_5NT_4NO_3]_n$ and $[Ag_5NT_4ClO_4]_n$ indicates their potential application as energetic oxidizers.

Introduction

Coordination polymers (CPs) have been shown to have many significant applications in the fields of chemistry and materials, including gas storage, sensors, and catalysis.[1] CPs have recently been used in high-energy-density materials (propellants, explosives, and pyrotechnics) and are known as energetic coordination polymers (ECPs).[2] According to their mechanical sensitivity, ECPs can be divided into primary and secondary explosives. Primary explosives are sensitive to external stimuli, such as impact, friction, and spark. The major role of primary explosives is to detonate powerful secondary explosives, which is quite important in military and civil applications.[3] Traditional primary explosives, including mercury fulminate, lead azide, and lead styphnate, have been widely used for over 100 years. However, the toxic properties of mercury and lead restrict their application.[4] Thus, new primary explosives must be developed.

A promising primary explosive must exhibit excellent initiation performance. For ECPs used as primary explosives, their ligands must be powerful. Among the heterocyclic rings used, tetrazoles have attracted much attention due to their high nitrogen content (>80%) and vast number of energy-rich N-N, C=N, and N=N bonds.[5] Several tetrazole-based compounds have been used to construct ECPs, such as 1-amino- and 2-amino-5H-tetrazoles, 5-(1-methylhydrazinyl)tetrazole, 1-methyl-5H-tetrazoles, 1H,1'H-5,5'-bitetrazole, 1H,1'H-[5,5'-bitetrazole]-1,1'-diol, di(1H-tetrazol-5-yl)methane, and N,N-bis(1H-tetrazol-5-yl)amine.[6] According to reported reseach, ECPs based on monotetrazoles always exhibit improved thermal stability as compared to those prepared using bitetrazoles. Meanwhile, monotetrazoles are easier to prepare than bitetrazoles. Thus, monotetrazoles are a good choice for the development of new ECPs for use as primary explosives.

Although many primary explosives based on tetrazoles have been reported, to the best of our knowledge, none of them exhibit a positive oxygen balance based on CO_2 (OB_{CO2}). In addition, when considering all of the ECPs-based primary explosives reported to date, there is also no literature-known case exhibiting a positive OB_{CO2}. Even extending to the whole metal-containing primary explosives, those with a positive

School of Chemical Engineering, Nanjing University of Science and Technology. Xiaolingwei 200, Nanjing, Jiangsu, China. E-mail: linqh@njust.edu.cn; luming@njust.edu.cn

† Footnotes relating to the title and/or authors should appear here.
Electronic Supplementary Information (ESI) available: [details of any supplementary information available should be included here]. See DOI: 10.1039/x0xx00000x

View Article Online
DOI: 10.1039/C9TA12506E

OB_{CO2} are also extremely rare.[7] It should be noted that ECPs with a zero or positive OB_{CO2} can convert all the carbon, hydrogen and metal atoms into carbon dioxide, water, and metal oxide, respectively. When compared with the ECPs displaying a negative OB_{CO2}, ECPs with a positive OB_{CO2} can generate less toxic gas, such as carbon monoxide. In addition, the oxygen generated during the decomposition of a primary explosive with a positive OB_{CO2} can also have a positive influence on the explosion of the secondary explosive. However, how to design and prepare primary explosives (ECPs) with a positive OB_{CO2} is a significant challenge.

Herein, to enrich the family of primary explosives with a positive OB_{CO2}, two strategies have been used to overcome the oxygen balance limitation: 1) By increasing the OB_{CO2} of the ligands; as shown in Scheme 1, the OB_{CO2} value from 5-MT to 5-NT increases from –114.2% to –7.0% (5-MT: 5-methyl-1-H-tetrazole, 5-HT: 5-hydrogen-1-H-tetrazole, 5-AT: 5-amino-1-H-tetrazole, and 5-NT: 5-nitro-1-H-tetrazole, respectively), and 2) the introduction of oxygen-rich ions (such as NO_3^- and ClO_4^-). As a result, three ECPs with a negative OB_{CO2}, *viz* $[Ag_7MT_4(NO_3)_3]_n$, $[Ag_3HT_2NO_3]_n$, and $[Ag_7AT_4(NO_3)_3]_n$ and two ECPs with a positive OB_{CO2}, *viz* $[Ag_5NT_4NO_3]_n$ and $[Ag_5NT_4ClO_4]_n$ were obtained. Their structures were characterized using single crystal XRD, IR, and elemental analysis. In addition, their properties were studied in terms of density, thermal stability, mechanical sensitivity and oxygen balance.

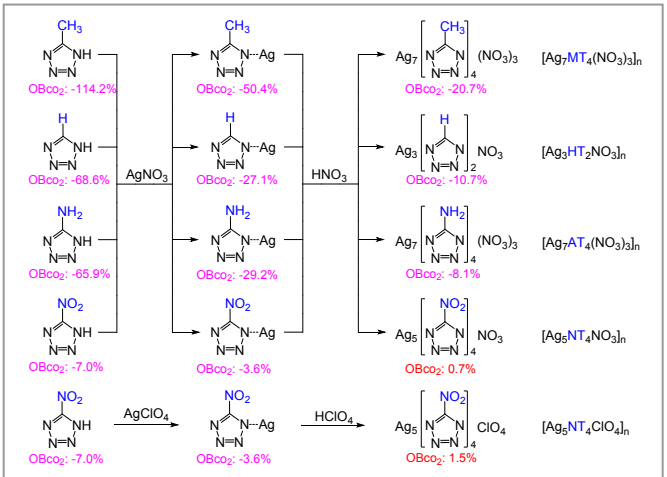

Scheme 1. Synthesis of five new ECPs. Oxygen balance of monotetrazoles and ECPs are indicated. (Purple: negative oxygen balance; Red: positive oxygen balance. The details of calculation of oxygen balance are provided in the section of oxygen balance).

Preparation and structures

Synthesis

To prepare the designed ECPs, 5-MT, 5-HT, 5-AT, and 5-NT, which display different oxygen balance values, were chosen to provide the tetrazole ligands, while silver nitrate was used to provide the metal node (Ag^+) and oxygen-rich anion (NO_3^-). The preparation process is presented in Scheme 1 and Figure 1. The addition of an aqueous solution of silver nitrate to a solution of the ligand (5-MT, 5-HT, 5-AT, and 5-NT, respectively) at 25 °C leads to the formation of a colorless precipitate. However, IR spectroscopy indicated that the as-obtained samples were AgMT, AgHT, AgAT, and AgNT, respectively, with no NO_3^- present in their structures. Furthermore, the introduction of NO_3^- was not accomplished upon changing the temperature, pressure, or molar ratio of the raw materials. To overcome this problem, nitric acid was added into the suspensions containing AgMT, AgHT, AgAT, and AgNT at 90 °C until a solution was formed. Keeping the temperature constant, crystals began to form after a few minutes. More crystals were obtained after the temperature decreased to room temperature. The resulting crystals were studied using single crystal X-ray diffraction, and the molecular formulas of the four resulting compounds were determined to be $[Ag_7MT_4(NO_3)_3]_n$, $[Ag_3HT_2NO_3]_n$, $[Ag_7AT_4(NO_3)_3]_n$, and $[Ag_5NT_4NO_3]_n$, respectively. As shown in Scheme 1, the introduction of NO_3^- increased the oxygen balance of the compounds. To further increase the oxygen balance, ClO_4^- was introduced into AgNT using the same method, and the X-ray data indicated its molecular formula was $[Ag_5NT_4ClO_4]_n$.

Crystal structures

In order to explore the potential relationships between the crystal structures of the five ECPs, they were divided into two groups: (1) $[Ag_7MT_4(NO_3)_3]_n$, $[Ag_3HT_2NO_3]_n$, $[Ag_7AT_4(NO_3)_3]_n$, and $[Ag_5NT_4NO_3]_n$, and (2) $[Ag_5NT_4NO_3]_n$ and $[Ag_5NT_4ClO_4]_n$.

For $[Ag_7MT_4(NO_3)_3]_n$, $[Ag_3HT_2NO_3]_n$, $[Ag_7AT_4(NO_3)_3]_n$, and $[Ag_5NT_4NO_3]_n$: Although all these four ECPs consist of silver, nitrate, and the tetrazole ligands, they show different crystal systems, which is mainly the result of the different tetrazole

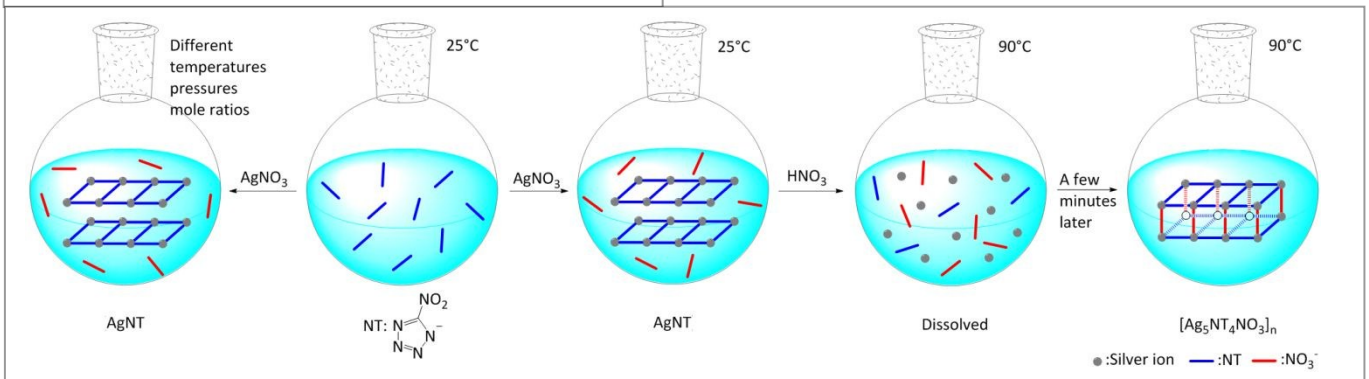

Figure 1. Preparation process of the five energetic coordination polymers. Taking $[Ag_5NT_4NO_3]_n$ as example.

View Article Online
DOI: 10.1039/C8TA12505E

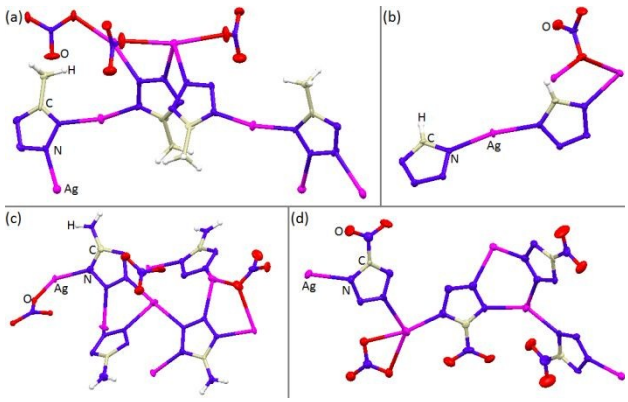

Figure 2. (a), (b), (c) and (d) Crystal structures for $[Ag_7MT_4(NO_3)_3]_n$, $[Ag_3HT_2NO_3]_n$, $[Ag_7AT_4(NO_3)_3]_n$, and $[Ag_5NT_4NO_3]_n$, respectively. White: H atoms, gray: C atoms, blue: N atoms, and purple: Ag atoms, respectively.

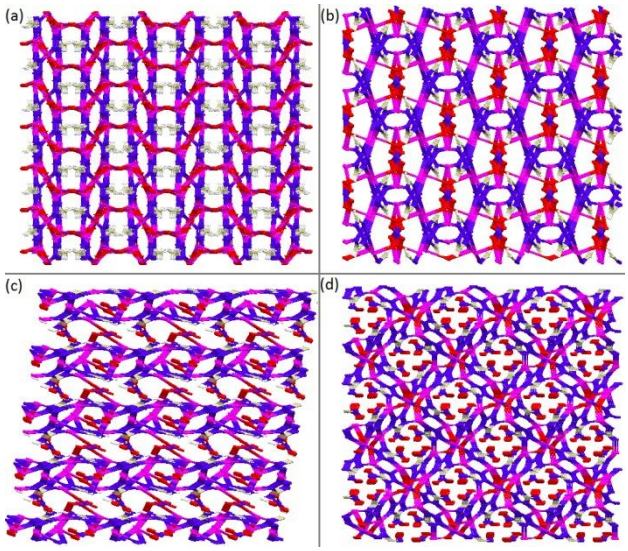

Figure 3. (a), (b), (c) and (d) Packing diagrams for $[Ag_7MT_4(NO_3)_3]_n$, $[Ag_3HT_2NO_3]_n$, $[Ag_7AT_4(NO_3)_3]_n$, and $[Ag_5NT_4NO_3]_n$, respectively.

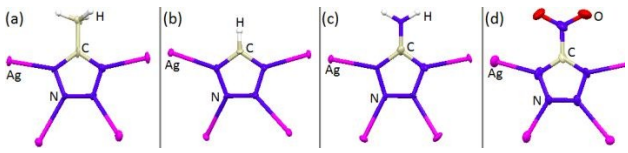

Figure 4. (a), (b), (c) and (d) Coordination environments of 5-MT, 5-HT, 5-AT, and 5-NT, respectively.

ligands used in their synthesis. As shown in Figure 2, one molecule of $[Ag_7MT_4(NO_3)_3]_n$ includes seven silver ions, three nitrate ions, and four MT ligands, which is different from $[Ag_3HT_2NO_3]_n$ and $[Ag_5NT_4NO_3]_n$, but the same as $[Ag_7AT_4(NO_3)_3]_n$. However, even though $[Ag_7MT_4(NO_3)_3]_n$ and $[Ag_7AT_4(NO_3)_3]_n$ possess the same molecular components, they still show different packing styles (Figures 3a and 3c) and different space groups (C2221 and P-1, respectively).

According to the X-ray data, it is interesting that all four tetrazole ligands are coordinated to four silver ions (Figure 4). The bond lengths observed for Ag-N in $[Ag_7MT_4(NO_3)_3]_n$ are 2.133–2.446 Å, and these values in $[Ag_3HT_2NO_3]_n$, $[Ag_7AT_4(NO_3)_3]_n$, and $[Ag_5NT_4NO_3]_n$ were 2.110–2.580 Å, 2.157–2.363 Å, and 2.223–2.487Å , respectively. There was no obvious tendency or rule for the bond lengths observed for Ag-N. In addition, the nitrate ions in these four coordination polymers are also coordinated to several silver ions, and the bond lengths observed for Ag-O are 2.283–2.283 Å, 2.290–2,570 Å, 2.623 Å, and 2.425–2.590 Å, respectively, which also do not show any obvious tendency or rule.

The packing diagrams of these four compounds are presented in Figure 5. The space groups of the four ECPs were C2221, C2/c, P-1, and Pn, and their crystal systems were orthorhombic, monoclinic, triclinic, and monoclinic, respectively. All of them exhibit rigid three-dimensional structures, which may exhibit a positive influence on the density and thermal stability of the ECPs.

For $[Ag_5NT_4NO_3]_n$ and $[Ag_5NT_4ClO_4]_n$: The molecular components of $[Ag_5NT_4NO_3]_n$ and $[Ag_5NT_4ClO_4]_n$ only differ by the presence of NO_3^- and ClO_4^-. The crystal structure and packing diagram of $[Ag_5NT_4ClO_4]_n$ are presented in Figure 5. Its

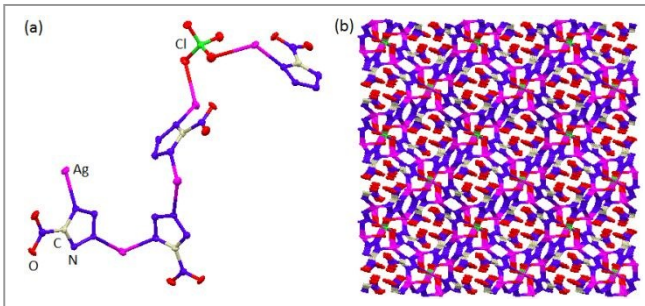

Figure 5. (a) Crystal structures for $[Ag_5NT_4ClO_4]_n$. (b) Packing diagrams for $[Ag_5NT_4ClO_4]_n$.

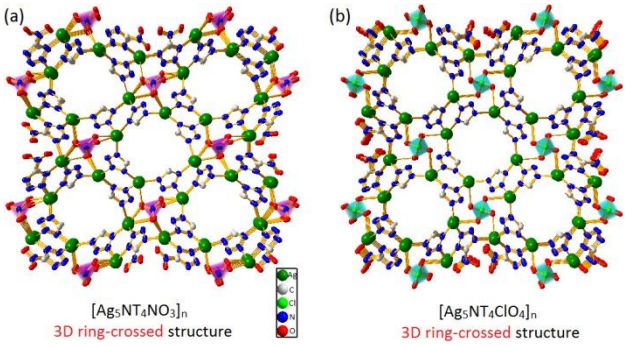

Figure 6. Packing diagrams of $[Ag_5NT_4NO_3]_n$ and $[Ag_5NT_4ClO_4]_n$ with Diamond program. Some nitro groups were deleted for clarification.

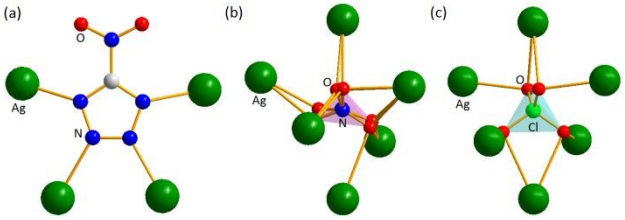

Figure 7. (a), (b), and (c) Coordination environments of 5-NT, NO_3^-, and ClO_4^-, respectively.

space group and crystal system are P42/n and tetragonal, respectively, which are different from those of $[Ag_5NT_4ClO_4]_n$.

It must be noted that $[Ag_5NT_4NO_3]_n$ and $[Ag_5NT_4ClO_4]_n$ exhibit very similar packing structures, which can be termed as a 3D ring-crossed structure. To compare their packing styles and structures more clearly, the packing diagrams were redrawn using the Diamond 3.2 program and presented in Figure 6, in which the NO_3^- ions were represented as purple polyhedra and ClO_4^- represented as turquoise polyhedra in the packing diagrams. Both packing structures observed for $[Ag_5NT_4NO_3]_n$ and $[Ag_5NT_4ClO_4]_n$ are composed of five rings in a crossed arrangement, and each ring consists of four oxygen-rich anions, eight silver ions, and eight 5-NT ligands. This phenomenon can be explained by the same coordination environments observed for 5-NT, NO_3^-, and ClO_4^-. The 5-NT ligands in these CPs are coordinated to four silver ions (Figure 7a), and the bond lengths observed for Ag-N were 2.223-2.487 Å and 2.204-2.445 Å, respectively. As shown in Figures 7(b) and 7(c), both the planar NO_3^- and tetrahedral ClO_4^- ions were coordinated to six silver ions. Furthermore, the positions of these silver ions were very similar. In addition, the bond lengths observed for Ag-O in $[Ag_5NT_4NO_3]_n$ and $[Ag_5NT_4ClO_4]_n$ are also very similar, that is, 2.425-2.590 Å and 2.581 Å, respectively.

Energetic properties

Density

The densities of the ECPs were obtained by converting the crystal density observed at 173 K to the crystal density at 298 K using an empirical equation.[8] In this case, due to the existence of the silver ions, the densities of the five ECPs were extremely high, and the values determined to be 3.26, 3.60, 3.58, 3.14, and 3.12 g cm^{-3}, respectively (Table 1). In addition, the densities were also determined by gas pycnometer, and the values are very close to the crystal data. For $[Ag_7MT_4(NO_3)_3]_n$, $[Ag_3HT_2NO_3]_n$, $[Ag_7AT_4(NO_3)_3]_n$, and $[Ag_5NT_4NO_3]_n$, although the densities of the ligands increase from 5-MT to 5-NT, those of the ECPs do not exhibit any particular tendency, which mainly results from the different molecular components. However, the densities are closely related to the silver content. For example, $[Ag_3HT_2NO_3]_n$ with the highest silver content shows the highest density, while $[Ag_5NT_4ClO_4]_n$ with the lowest silver content shows the lowest density. However, for $[Ag_7MT_4(NO_3)_3]_n$ and $[Ag_7AT_4(NO_3)_3]_n$, their silver content is very similar, but their densities are quite different. To better understand the density, the packing coefficient (PC) of these ECPs were studied. It is clear that the PC of $[Ag_7AT_4(NO_3)_3]_n$ is much higher than that of $[Ag_7MT_4(NO_3)_3]_n$, which caused $[Ag_7AT_4(NO_3)_3]_n$ to exhibit a higher density. In addition, although the PC of $[Ag_3HT_2NO_3]_n$ is slightly lower than that of $[Ag_7AT_4(NO_3)_3]_n$, its density is the highest, which mainly results from its highest silver content. So, it can be concluded that the densities of these ECPs are closely related to the silver content and packing coefficient.

Thermal stability

Thermal stability is one of the most important properties of an energetic material. In general, energetic materials, which can be used in practical applications, should exhibit a decomposition temperature of >200 °C.[9] In this study, differential scanning calorimetry (DSC) and thermogravimetric analysis (TGA) were used to evaluate the thermal stability of the five ECPs. The DSC plots are shown in Figure 8, while the TGA plots are presented in the ESI. $[Ag_7MT_4(NO_3)_3]_n$, $[Ag_3HT_2NO_3]_n$, $[Ag_7AT_4(NO_3)_3]_n$, $[Ag_5NT_4NO_3]_n$, and $[Ag_5NT_4ClO_4]_n$ possess very high onset decomposition temperatures of 348, 251, 307, 312, and 306 °C, respectively. It should be noted that the decomposition temperature of $[Ag_7MT_4(NO_3)_3]_n$ was extremely high (348 °C), which is higher than mainstream heat-resistant explosives, such as hexanitrostilbene (HNS, T_d: 316 °C), 2,4,6-triamino-1,3,5-trinitrobenzene (TATB, T_d: 330 °C) and 5,5 ' -bis(2,4,6-trinitrophenyl)-2,2 ' -bi(1,3,4-oxadiazole) (TKX-55, T_d: 335 °C), but slightly lower than ,6-bis(picrylamino)-3,5-dinitropyridine (PYX, T_d: 357 °C).[10] Therefore, $[Ag_7MT_4(NO_3)_3]_n$ shows great potential as a new heat-resistant explosive. The good thermal stability of the ECPs can be attributed to the

Table 1 Density parameters of five energetic coordination polymers.

Compd	d_1[a]	d_2[b]	d_3[c]	Ag[d]	PC[e]
	g cm^{-3}	g cm^{-3}	g cm^{-3}	%	%
$[Ag_7MT_4(NO_3)_3]_n$	3.26	3.24	1.32	59.3	73.1
$[Ag_3HT_2NO_3]_n$	3.60	3.59	1.48	61.8	78.3
$[Ag_7AT_4(NO_3)_3]_n$	3.58	3.56	1.50	59.1	78.4
$[Ag_5NT_4NO_3]_n$	3.14	3.14	1.85	51.0	75.3
$[Ag_5NT_4ClO_4]_n$	3.12	3.11	1.85	49.3	75.1

[a] Density of coordination polymers. Crystal density at 298 K. $d_{298K}=d_T/(1+\alpha_v(298-T))$; $\alpha_v=1.5\times10^{-4}$ K^{-1}, T equals to the testing temperature. [b] Density of coordination polymers measured by gas pycnometer, 298 K. [c]Density of tetrazole ligands. [d] Content of silver. [e] Packing coefficient.

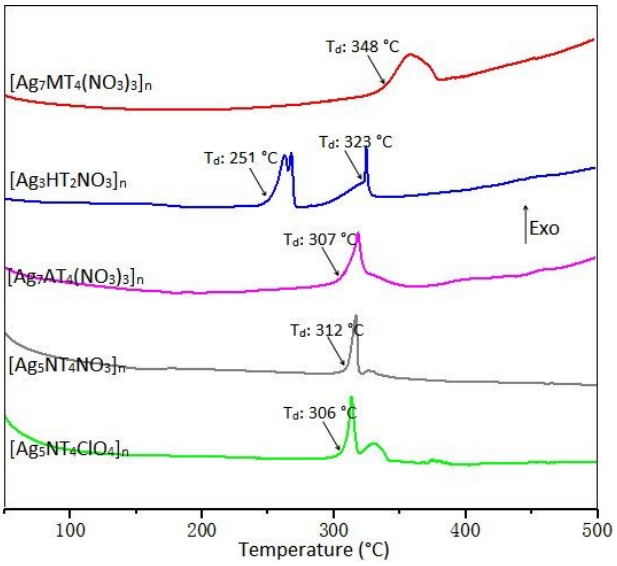

Figure 8. DSC plots for $[Ag_7MT_4(NO_3)_3]_n$, $[Ag_3HT_2NO_3]_n$, $[Ag_7AT_4(NO_3)_3]_n$, $[Ag_5NT_4NO_3]_n$, and $[Ag_5NT_4ClO_4]_n$, respectively.

View Article Online
DOI: 10.1039/C9TA12506E

Table 2. Sensitivity parameters of five energetic coordination polymers.

Compd	IS[a] [J]	FS[b] [N]	ESD[c] [mJ]
$[Ag_7MT_4(NO_3)_3]_n$	5	60	100
$[Ag_3HT_2NO_3]_n$	2	10	40
$[Ag_7AT_4(NO_3)_3]_n$	4	20	60
$[Ag_5NT_4NO_3]_n$	1	5	10
$[Ag_5NT_4ClO_4]_n$	1	2	5
Lead styphnate[d]	2.5-5	1.5	0.02-1.0
Lead azide[d]	2.5-4	0.1-1	6-12

[a] Impact sensitivity. [b] Friction sensitivity. [c] Electrostatic discharge sensitivity. [d] Ref 6a.

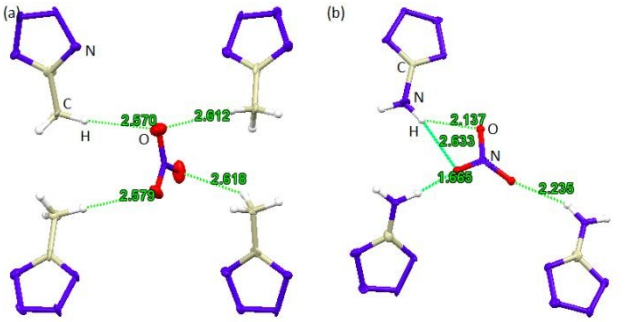

Figure 9. Hydrogen-bonding interactions (a) between 5-MT and NO_3^-, (b) between 5-AT and NO_3^-.

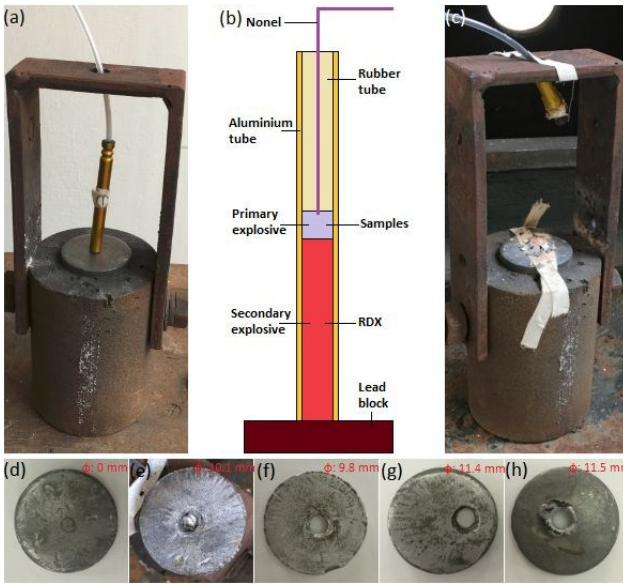

Figure 10. (a) Equipment for the test of initiation performance before explosion. (b) Schematic diagram for the explosion experiment. (c) Equipment for the test of initiation performance after explosion. (d), (e), (f), (g), and (h) The lead blocks after explosions initiated by 50 mg primary explosive, $[Ag_7MT_4(NO_3)_3]_n$, $[Ag_3HT_2NO_3]_n$, $[Ag_7AT_4(NO_3)_3]_n$, $[Ag_5NT_4NO_3]_n$, and $[Ag_5NT_4ClO_4]_n$, respectively.

following two reasons: (1) The high molecular stability of the monotetrazole ligands and (2) the strong structural reinforcement in the 3D framework. In addition, to better understand their different thermal stability, the bond dissociation energies (BDEs) of trigger bonds of ligands are studied (ESI). The calculation indicates that 5-MT possesses the highest BDE, which may lead $[Ag_7MT_4(NO_3)_3]_n$ to exhibit the best thermal stability. While 5-NT exhibits the lowest BDE, but $[Ag_5NT_4NO_3]_n$ and $[Ag_5NT_4ClO_4]_n$ do not show the worst thermal stability. In other words, the thermal stability of the ECPs is not determined only by the BDEs of the ligands, but may be related to many other factors, such as hydrogen bonds, packing styles, and so on.

Mechanical sensitivity

As mentioned in the introduction, ECPs can be divided into primary and secondary explosives according to their mechanical sensitivity. In this study, the sensitivity of the ECPs towards impact and friction were determined using the standard BAM methods, and the electrostatic discharge sensitivity was also assessed.[11] The results shown in Table 2 indicate that all of the ECPs were sensitive to external stimuli and should be classified as primary explosives. $[Ag_5NT_4NO_3]_n$ and $[Ag_5NT_4ClO_4]_n$ exhibited very sensitive properties (IS: 1 and 1 J, FS: 5 and 2 N, and ESD: 10 and 5 mJ, respectively), while the other three ECPs showed lower mechanical sensitivity. This difference mainly results from three reasons: 1) The different properties of the functional groups: $-CH_3$ and $-NH_2$ are stabilizing groups, while $-NO_2$ is a powerful energetic groups; 2) the difference in hydrogen bonds: $[Ag_7MT_4(NO_3)_3]_n$ and $[Ag_7AT_4(NO_3)_3]_n$ exhibit relatively good mechanical sensitivity, which can be attributed to the hydrogen-bonding interactions between $-NH_2$ and NO_3^- (Figure 9); and 3) the different packing styles: the packing diagrams of these five ECPs without metal nodes were presented in ESI. It was found that $[Ag_7MT_4(NO_3)_3]_n$, $[Ag_3HT_2NO_3]_n$, and $[Ag_7AT_4(NO_3)_3]_n$ exhibit face-to-face stacking, while $[Ag_5NT_4NO_3]_n$ and $[Ag_5NT_4ClO_4]_n$ exhibit wavelike stacking. Previous studies indicate that face-to-face stacking possesses a higher maximum limit than wavelike stacking, which means compounds featuring face-to-face stacking may have better mechanical sensitivities than compounds featuring wavelike stacking.

Explosion experiments were conducted to compare the initiation performance of these primary explosives. The equipment before explosion, schematic diagrams, and equipment after the explosion are presented in Figures 10(a), (b), and (c), respectively. The five primary explosives (50 mg) and RDX (400 mg) were loaded into an aluminum tube, which was then connected with the nonel. The aluminum tube was placed on a lead block and then detonated using an electric firing igniter. After the explosion, it was found that the aluminum tube was broken. The lead blocks after the explosions generated using the different primary explosives are shown in Figures 10(d), (e), (f), (g), and (h), respectively. The results indicate that RDX can be detonated using $[Ag_3HT_2NO_3]_n$, $[Ag_7AT_4(NO_3)_3]_n$, $[Ag_5NT_4NO_3]_n$, and $[Ag_5NT_4ClO_4]_n$, and not by $[Ag_7MT_4(NO_3)_3]_n$. This means $[Ag_3HT_2NO_3]_n$, $[Ag_7AT_4(NO_3)_3]_n$,

View Article Online
DOI: 10.1039/C8TA12500F

$[Ag_5NT_4NO_3]_n$, and $[Ag_5NT_4ClO_4]_n$ are effective primary explosives. To further compare their initiation performance, the diameters of these holes were measured. It is clear that the holes generated by $[Ag_5NT_4NO_3]_n$ and $[Ag_5NT_4ClO_4]_n$ are larger than the other three primary explosives, which indicate that $[Ag_5NT_4NO_3]_n$ and $[Ag_5NT_4ClO_4]_n$ show an enhanced initiation performance than the other three primary explosives.

Oxygen balance

The oxygen balance is important when considering the decomposition products of energetic materials. It must be noted that because of the uncertainty of the detonation products of metals, there is no standard method used to calculate the oxygen balance of metal-containing energetic materials. However, the most conventional method used assumes that the metals are converted into metal oxides. In this study, the OB_{CO2} value for $C_aH_bO_cN_dAg_e$ is equal to 1600(c-2a-b/2-e/2)/M_w, and the values for $[Ag_7MT_4(NO_3)_3]_n$, $[Ag_3HT_2NO_3]_n$, $[Ag_7AT_4(NO_3)_3]_n$, and $[Ag_5NT_4NO_3]_n$ were determined to be –20.7, –10.7, –8.1, and 0.7%, respectively. While for $C_aH_bO_cN_dAg_eCl_f$, the Cl atoms are assumed to be converted into AgCl, and OB_{CO2} is equal to 1600[c-2a-b/2-(e-f)/2]/M_w. The value for $[Ag_5NT_4ClO_4]_n$ was determined to be 1.5%. It is interesting that the OB_{CO2} increases from $[Ag_7MT_4(NO_3)_3]_n$ to $[Ag_5NT_4NO_3]_n$, and this tendency is the same as the OB_{CO2} increase observed from 5-MT to 5-NT. The change from NO_3^- to ClO_4^- also leads to the increase in OB_{CO2} observed from $[Ag_5NT_4NO_3]_n$ to $[Ag_5NT_4ClO_4]_n$.

It must be pointed out that the OB_{CO2} of $[Ag_5NT_4NO_3]_n$ and $[Ag_5NT_4ClO_4]_n$ are positive. To the best of our knowledge, this is a great advance because there is no ECPs-based primary explosive with a positive OB_{CO2} reported to date. Even extending to the whole metal-containing primary explosives, there are only two cases exhibiting a positive OB_{CO2}. Because of the particularity of these two compounds, and the uncertainty of the calculation methods used to determine the oxygen balance of metal-containing energetic materials, theoretical analysis and practical combustion experiments were conducted to confirm whether $[Ag_5NT_4NO_3]_n$ and $[Ag_5NT_4ClO_4]_n$ exhibit a positive OB_{CO2}.

According to H_2O-CO_2 arbitrary theory, the detonation reactions observed for these compounds are presented in Scheme 3.[12] For $[Ag_7MT_4(NO_3)_3]_n$, $[Ag_3HT_2NO_3]_n$, and $[Ag_7AT_4(NO_3)_3]_n$, it is clear that the number of O atoms is not sufficient to oxidize the Ag and C atoms to form Ag_2O and CO_2, which means these three compounds show a negative OB_{CO2} and no O_2 is generated in their decomposition. However, for $[Ag_5NT_4NO_3]_n$ and $[Ag_5NT_4ClO_4]_n$, the number of O atoms is sufficient enough to oxidize the C and Ag atoms to CO_2 and Ag_2O. Furthermore, there is additional O_2 generated, meaning that $[Ag_5NT_4NO_3]_n$ and $[Ag_5NT_4ClO_4]_n$ exhibit a positive OB_{CO2}.

If energetic compounds exhibit a positive oxygen balance, they can be used as energetic oxidizers. Thus, the combustion experiments of $[Ag_5NT_4NO_3]_n$ and $[Ag_5NT_4ClO_4]_n$ were performed. The samples were ignited and recorded using a high-speed camera (2000 fps s^{-1}). The fuel chosen was nanoscale aluminum powder, because it cannot be ignited in air without an oxidizer. The combustion performance of the two different samples (a: Al and $[Ag_5NT_4NO_3]_n$; b: Al and $[Ag_5NT_4ClO_4]_n$) is presented in Figure 11. The interval time per picture was 5 μs. The burning time for (a) was 115 μs, while for (b) it was 100 μs. It is clear that the burning processes of (b) is more rapid and violent than (a), which means $[Ag_5NT_4ClO_4]_n$ exhibits enhanced oxidizability when compared to $[Ag_5NT_4NO_3]_n$. The fact that aluminum powder can be successfully ignited indicates that $[Ag_5NT_4NO_3]_n$ and $[Ag_5NT_4ClO_4]_n$ are effective oxidizers. In other words, they do exhibit a positive oxygen balance.

$Ag_7C_8H_{12}N_{19}O_9 = 7Ag + 1.5CO_2 + 6H_2O + 9.5N_2 + 6.5C$ $[Ag_7MT_4(NO_3)_3]_n$

$Ag_3C_2H_2N_9O_3 = 3Ag + CO_2 + H_2O + 4.5N_2 + C$ $[Ag_3HT_2NO_3]_n$

$Ag_7C_4H_8N_{23}O_9 = 7Ag + 2.5CO_2 + 4H_2O + 11.5N_2 + 1.5C$ $[Ag_7AT_4(NO_3)_3]_n$

$Ag_5C_4N_{21}O_{11} = 2.5Ag_2O + 4CO_2 + 10.5N_2 + 0.5O_2$ $[Ag_5NT_4NO_3]_n$

$Ag_5C_4ClN_{20}O_{12} = 2Ag_2O + AgCl + 4CO_2 + 10N_2 + O_2$ $[Ag_5NT_4ClO_4]_n$

Scheme 3. Detonation reactions of five energetic coordination polymers.

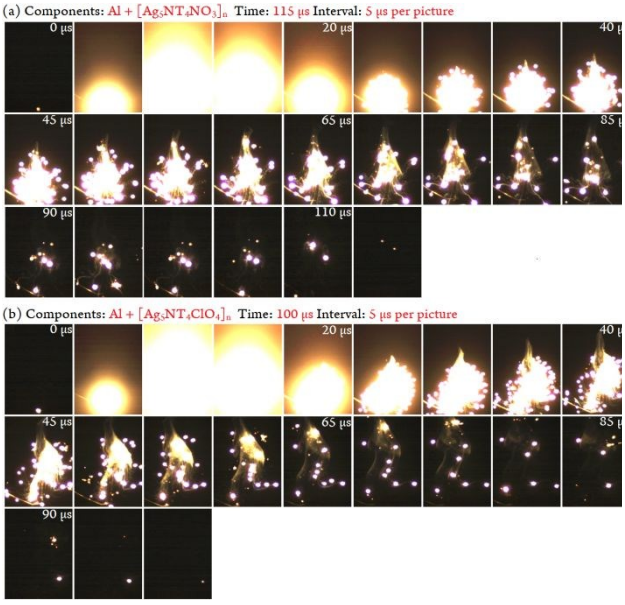

Figure 11. Combustion performance of different samples. (a) Al and $[Ag_5NT_4NO_3]_n$. (b) Al and $[Ag_5NT_4ClO_4]_n$.

Conclusions

In summary, a series of energetic coordination polymers, $[Ag_7MT_4(NO_3)_3]_n$, $[Ag_3HT_2NO_3]_n$, $[Ag_7AT_4(NO_3)_3]_n$, $[Ag_5NT_4NO_3]_n$, and $[Ag_5NT_4ClO_4]_n$, have been presented. The materials were synthesized from 5-substituted monotetrazoles upon coordination with silver and oxygen-rich ions using a simple and facile synthesis process. The structures of the ECPs were confirmed using single crystal X-ray diffraction, IR, and element analysis. The densities of the ECPs fall in the range of 3.12–3.60 g cm^{-3}, and are closely related to the silver content and packing coefficient. The high thermal stability with decomposition temperatures from 251 to 348 °C can be attributed to the high molecular stability of the monotetrazole ligands and the strong

DOI: 10.1039/C8TA12505E

structural reinforcement of the 3D framework. It should be noted that $[Ag_7MT_4(NO_3)_3]_n$ exhibits a decomposition temperature of 348 °C, which is higher than the mainstream heat-resistant explosives, such as HNS, TATB, and TKX-55. The mechanical sensitivity indicates that the ECPs are primary explosives. In particular, $[Ag_5NT_4NO_3]_n$ and $[Ag_5NT_4ClO_4]_n$ exhibit very sensitive properties (IS: 1 and 1 J, FS: 5 and 2 N, and ESD: 10 and 5 mJ, respectively), which are more sensitive than the other three ECPs. Such a difference results from the different properties of the functional groups, different non-covalent interactions (hydrogen-bonding interactions), and different packing styles. It is worth pointing out that $[Ag_5NT_4NO_3]_n$ and $[Ag_5NT_4ClO_4]_n$ exhibit a positive oxygen balance (based on CO_2), which was confirmed using three different methods: Oxygen balance calculations, detonation reactions, and combustion experiments. This is a great advance because there is no literature-known ECPs-based primary explosive exhibiting a positive oxygen balance (based on CO_2). The explosion experiments also indicate that $[Ag_5NT_4NO_3]_n$ and $[Ag_5NT_4ClO_4]_n$, which have a positive oxygen balance show better initiation performance than $[Ag_7MT_4(NO_3)_3]_n$, $[Ag_3HT_2NO_3]_n$, and $[Ag_7AT_4(NO_3)_3]_n$, which have a negative oxygen balance. We believe this work can give new insight to tetrazoles, coordination polymers, and energetic materials (primary explosives).

Experimental section

Attention

Compounds presented in this study are sensitive primary explosives. Although there were no explosion found in our operation, careful treatments and safety protections are encouraged.

Syntheses

General methods on preparing AgMT, AgHT, AgAT, and AgNT.

NaMT (1.06 g, 10 mmol), NaHT (0.92 g, 10 mmol), NaAT (1.07 g, 10 mmol), or NaNT (1.37 g, 10 mmol), was dissolved in 20 ml water, and silver nitrate (1.70 g, 10 mmol) dissolved in water was slowly added. After stirring for 10 min at room temperature, the white solid was collected by filtration, washed with water, and dried in air to obtain AgMT (1.84 g, 96.3% yield), AgHT (1.74 g, 98.1% yield), AgAT (1.87 g, 97.4% yield), and AgNT (2.15 g, 97.7% yield).

General methods on preparing $[Ag_7MT_4(NO_3)_3]_n$, $[Ag_3HT_2NO_3]_n$, $[Ag_7AT_4(NO_3)_3]_n$, and $[Ag_5NT_4NO_3]_n$.

AgMT (0.95 g, 5 mmol), AgHT (0.88 g, 5 mmol), AgAT (0.96 g, 5 mmol), or AgNT (1.10 g, 5 mmol) was dispersed in 50 ml water at room temperature. Rising the temperature to 90 °C, nitric acid (68%) was added until the mixture turned into clear solution. Keeping the temperature constant, the precipitate appeared after a few minutes. More solid would be obtained, if the temperature fall to room temperature. The white solid was collected by filtration, washed with water, and dried in air to give $[Ag_7MT_4(NO_3)_3]_n$ (0.63 g, 69.3% yield), $[Ag_3HT_2NO_3]_n$ (0.44 g, 50.4% yield), $[Ag_7AT_4(NO_3)_3]_n$ (0.59 g, 64.7% yield), or $[Ag_5NT_4NO_3]_n$ (0.53 g, 50.1% yield).

$[Ag_7MT_4(NO_3)_3]_n$: IR (KBr): 1496 1381 1373 1226 1135 1109 1092 1033 706 697 cm^{-1}. Elemental analysis calcd for $Ag_7C_8H_{21}N_{19}O_9$ (1273.39): C 7.55, H 0.95, N 20.90 %; found C 7.39, H 0.88, N 21.11 %.

$[Ag_3HT_2NO_3]_n$: IR (KBr): 3132 1441 1325 1313 1208 1138 1106 1032 1014 911 815 686 cm^{-1}. Elemental analysis calcd for $Ag_3C_2H_2N_9O_3$ (523.70): C 4.59, H 0.38, N 24.07 %; found C 4.41, H 0.32, N 24.19 %.

$[Ag_7AT_4(NO_3)_3]_n$: IR (KBr): 3425 3355 1633 1453 1371 1280 1188 1167 1077 1037 814 779 737 cm^{-1}. Elemental analysis calcd for $Ag_7C_4H_8N_{23}O_9$ (1277.34): C 3.76, H 0.63, N 25.22 %; found C 3.55, H 0.58, N 25.39 %.

$[Ag_5NT_4NO_3]_n$: IR (KBr): 1551 1493 1455 1427 1322 1203 1171 1076 1040 832 810 658 cm^{-1}. Elemental analysis calcd for $C_4Ag_5N_{21}O_{11}$ (1057.60): C 4.54, N 31.56 %; found C 4.29, N 31.41 %.

Methods on preparing $[Ag_5NT_4ClO_4]_n$.

AgNT (1.10 g, 5 mmol) was dispersed in 50 ml water at room temperature. Rising the temperature to 90 °C, perchloric acid (60%) was added until the mixture turned into clear solution. Keeping the temperature constant, the precipitate appeared after a few minutes. More solid would be obtained, if the temperature fall to room temperature. The white solid was collected by filtration, washed with water, and dried in air to give $[Ag_5NT_4ClO_4]_n$ (0.43 g, 39,3%).

$[Ag_5NT_4ClO_4]_n$: IR (KBr): 1551 1494 1454 1425 1319 1205 1169 1061 832 769 660 622 610 cm^{-1}. Elemental analysis calcd for $C_4Ag_5ClN_{20}O_{12}$ (1095.04): C 4.39, N 25.58 %; found C 4.52, N 25.43 %.

Conflicts of interest

There are no conflicts to declare.

Acknowledgements

We gratefully acknowledge financial support from the National Natural Science Foundation of China (NSAF, No. U1530101 and NSFC, No. 21805138). The authors gratefully acknowledge Dr Zaichao Zhang (Huaiyin Normal University, China) for his analysis of the crystal structures.

Notes and references

1 (a) J. T. Damron, J. Liu, R. Kurz, K. Saalwachter, A. J. Matzger, *Angew. Chem. Int. Ed.* **2018**, 57, 8678-8681; (b) K. Sabyrov, J. Jiang, O. M. Yaghi, G. A. Somorjai, *J. Am. Chem. Soc*., **2017**, 139, 12382−12385; (c) M. J. Kalmutzki, C. S. Diercks, O. M. Yaghi, *Adv. Mater*., **2018**, 30, 1704304; (d) Y. Zhang, X. Zhang, J. Lyu, K. Otake, X. Wang, L. R. Redfern, C. D. Malliakas, Z. Li, T. Islamoglu, B. Wang and O. K. Farha, *J. Am. Chem. Soc.*, **2018**, 140, 11179−11183; (e) K. L. M. Harriman, J. L. Brosmer, L. Ungur, P. L. Diaconescu, M. Murugesu, *J. Am. Chem. Soc*., **2017**, 39, 1420 − 1423.

2 (a) S. Li, Y. Wang, C. Qi, X. Zhao, J Zhang, S. Zhang, S. Pang, *Angew. Chem. Int. Ed.* **2013**, 52, 14031-14035; (b) S. Seth, A. J. Matzger, *Inorg. Chem*. 2017, 56, 561−565; (c) Q. Wang, S. Wang, X. Feng, L. Wu, G. Zhang, M. Zhou, B. Wang, L. Yang, *ACS Appl. Mater. Interfaces* **2017**, 9, 37542−37547.

3 K. A. Mcdonald, S. Seth, A. J. Matzger, Cryst. Growth Des. 2015, 15, 5963−5972.

4 (a) Y. Tang, C. He, D. A. Mitchell, J. M. Shreeve, *Angew. Chem. Int. Ed.* **2016**, 55, 5565-5567; (b) D. Chen, H. Yang, Z. Yi, H. Xiong, S. Zhu, G. Zhu, *Angew. Chem. Int. Ed*. **2018**, 57, 2081-2084; (c) Q. Sun, Y. Liu, X. Li, M. Lu, Q. Lin, *Chem. Eur. J.* **2018**, 24, 14213-14219.

5 (a) T. M. Klapötke, F. A. Martin, J. Stierstorfer, *Angew. Chem., Int. Ed.* **2011**, 50, 4227−4229; (b) Q. Sun, C. Shen, X. Li, Q. Lin

View Article Online
DOI: 10.1039/C8TA12506F

and M. Lu, *Cryst. Growth Des*., **2017**, 17, 6105-6110; (c) B. Wang, X. Qi, W. Zhang, K. Wang, W. Li, Q. Zhang, *J. Mater. Chem. A*, **2017**, 5, 20867-20873; (d) T. M. Klapötke, J. Stierstorfer, *J. Am. Chem. Soc*. **2009**, 131, 1122 – 1134

6 (a) N. Szimhardt, M. H. H. Wurzenberger, L. Zeisel, M. S. Gruhne, M. Lommel, J. Stierstorfer, *J. Mater. Chem. A*, **2018**, 6, 16257-16272; (b) Z. Guo, Y. Wu, C. Deng, G. Yang, J. Zhang, Z. Sun, H. Ma, C. Gao, Z. An, *Inorg. Chem*. **2016**, 55, 11064−11071; (c) M. Freis, T. M. Klapötke, J. Stierstorfer, N. Szimhardt, *Inorg. Chem*. 2017, 56, 7936 – 7947; (d) G. Tao, D. A. Parrish, J. M. Shreeve, *Inorg. Chem*. **2012**, 51, 5305−5312; (e) F. Li, Y. Bi, W. Zhao, T. Zhang, Z. Zhou, L. Yang, *Inorg. Chem.* 2015, 54, 2050−2057; (f) G. Tao, B. Twamley, J. M. Shreeve, *Inorg. Chem*. **2009**, 48, 5305−5312;

7 (a) C. He, J. M. Shreeve, *Angew. Chem., Int. Ed*. **2016**, 55, 772 – 775; (b) D. Fischer, T. M. Klapötke, J. Stierstorfer, *Angew. Chem., Int. Ed.* **2015**, 54, 10299–10302.

8 (a) Q. Sun, Q. Lin and M. Lu, *CrystEngComm*, **2018**, 20, 4321-4328; (b) Q. Sun, Q. Lin and M. Lu, *Org. Biomol. Chem*., **2018**, 16, 8034 – 8037.

9 (a) C. Bian, M. Zhang, C. Li, Z. Zhou, J. Mater. Chem. A, 2015, 3, 163-169; (b) D. E. Chavez, D. A. Parrish, L. Mitchell, G. H. Imler, Angew.Chem. Int.Ed. 2017, 56, 3575-3578; (c) Y. Tang, D. Kumar, J. M. Shreeve, J. Am. Chem. Soc. 2017, 139, 13684−13687.

10 (a) T. M. Klapötke, T. G. Witkowski, *ChemPlusChem*, **2016**, 81, 357 -360; (b) K. G. Shipp, *J. Org. Chem.* **1964**, 29, 2620-2623; (c) J. P. Agrawal, U. S. Prasad, R. N. Surve, *New J. Chem*. **2000**, 24, 583-585; (d) Q. Sun, C. Shen, X. Li, Q. Lin, M. Lu, J. Mater. Chem. A 2017, 5, 11063−11070;

11 Tests were conducted according to the UN Recommendations on the Transport of Dangerous Goods, Manual of Tests and Criteria, 5th ed.; United Nations: New York, **2009**.

12 (a) C. Shen, Y. Liu, Z. Zhu, Y. Xu, M. Lu, *Chem. Commun*., **2017**, 53, 7489-7492; ; (c) J. Xu, C. Sun, M. Zhang, B. Liu, X. Li, J. Lu, S. Wang, F. Zheng, G. Guo, *Chem. Mater.* **2017**, 29, 9725-9733.

View Article Online
DOI: 10.1039/C8TA12506F

$[Ag_5NT_4NO_3]_n$ and $[Ag_5NT_4ClO_4]_n$

ECPs-based primary explosives with positive oxygen balance

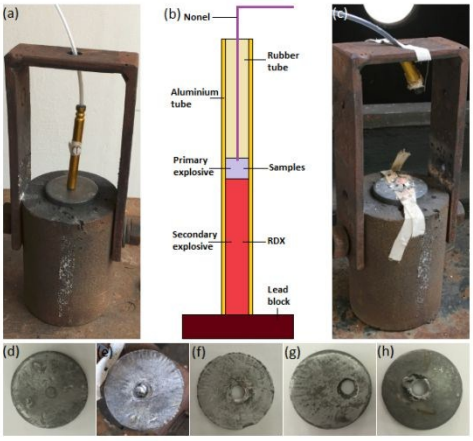

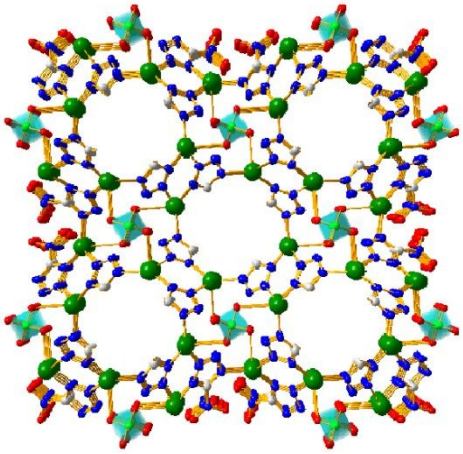

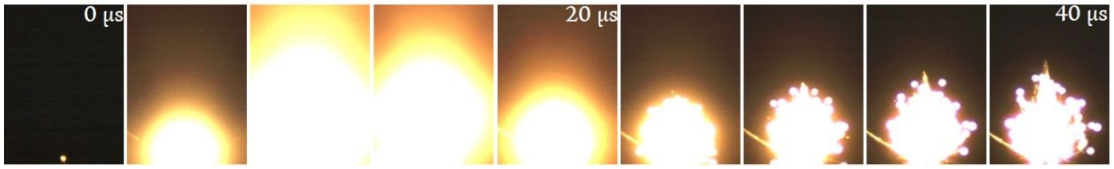

The first two examples of ECPs-based primary explosives exhibiting a positive oxygen balance (based on CO_2), $[Ag_5NT_4NO_3]n$ and $[Ag_5NT_4ClO_4]_n$, were presented.